ACS EARTH AND SPACE CHEMISTRY

ACS AUTHORCHOICE

http://pubs.acs.org/journal/aesccq

Article

Exploring the Maze of $C_2N_2H_5$ Radicals and Their Fragments in the Interstellar Medium with the Help of Quantum-Chemical Computations

Zoi Salta, Nicola Tasinato,* Jacopo Lupi, Rahma Boussessi, Alice Balbi, Cristina Puzzarini, and Vincenzo Barone

Cite This: *ACS Earth Space Chem.* 2020, 4, 774–782

Read Online

ACCESS | Metrics & More | Article Recommendations | Supporting Information

ABSTRACT: Among the species discovered in the interstellar medium and planetary atmospheres, a crucial role is played by the so-called "interstellar" complex organic molecules (iCOMs) because they are the signature of the increasing molecular complexity in space. Indeed, they may represent the connection between simple molecules and biochemical species like amino acids and nucleobases. In particular, HCN and the related CN radical are the starting points of rich nitrile chemistry. In this framework, we have undertaken a computational investigation of the gas-phase reaction mechanisms involving different $C_2N_2H_5$ radicals and their fragments, stemming from the addition of the cyano radical to the nitrogen atom of methylamine. Aiming at exploiting an accurate yet cost-effective protocol, a combination of CCSD(T)-based composite schemes and density functional theory has been employed. The exploration of the plausible chemical reaction channels has led to the identification of 12 different products, as well as 28 transition states connecting reactants, intermediates, and products. Aminoacetonitrile (H_2NCH_2CN), proposed as an intermediate in the formation of the smallest amino acid glycine, and the CH_2NH_2 radical appear as products energetically accessible under astrophysical conditions.

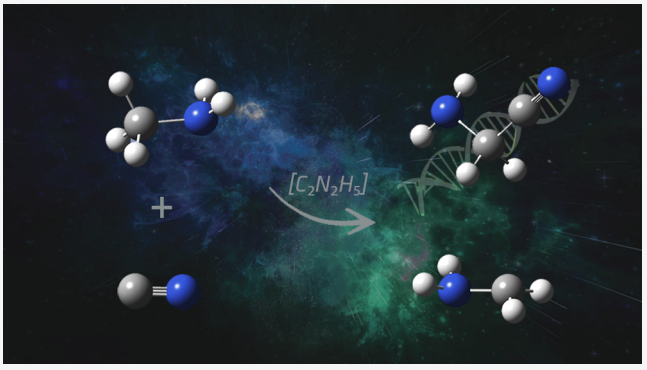

KEYWORDS: *astrochemistry, reaction network, nitrile radicals, aminoacetonitrile formation route, quantum chemistry*

1. INTRODUCTION

Since the early 1960s, the discovery of new molecules in the interstellar medium (ISM) has continued at a nearly steady pace.[1] However, in the last decade, the rate of detection of new interstellar complex organic molecules (iCOMs) has been further accelerating.[1] The importance of these species lies in the evidence, accumulated in the last decades, that iCOMs play the key role of precursors of biochemical building blocks, either in outer space or in planetary atmospheres resembling that of the primordial earth.[2−4] To give an example of the molecular complexity characterizing the interstellar medium (ISM), arcsecond resolution interferometry with the Berkeley−Illinois−Maryland Association (BIMA) array resulted in the detection and imaging of many iCOMs in the proximity of the "Large Molecule Heimat" (LMH) hot core—located in the Sagittarius B2(N) molecular cloud—such as vinyl cyanide (CH_2CHCN), methyl formate ($HCOOCH_3$), ethyl cyanide (CH_3CH_2CN), formamide (NH_2CHO), isocyanic acid (HNCO), acetic acid (CH_3COOH), formic acid (HCOOH), and acetone ($(CH_3)_2CO$),[5−11] all products of a complex and not yet fully elucidated chemistry.

The rich organic chemistry discovered in molecular clouds[12,13] has stimulated further efforts to detect even more complex species of prebiotic interest.[14] In turn, the evidence for molecular complexity has led to the need for a deeper rationalization of the chemical evolutionary steps operating in the ISM or in planetary atmospheres. Among iCOMs, the compounds containing the cyano moiety (CN functional group) can be surely numbered among the most important prebiotic molecules because they are potential precursors of amino acids, the main constituents of proteins, and of nucleobases, the fundamental components of DNA and RNA.[3,15] The search for amino acids (and their precursors) is indeed one of the most exciting challenges and opens questions for modern astronomy and astrophysics, also having

Received: March 6, 2020
Revised: March 31, 2020
Accepted: April 1, 2020
Published: April 1, 2020

https://dx.doi.org/10.1021/acsearthspacechem.0c00062
ACS Earth Space Chem. 2020, 4, 774–782

astrobiological implications with respect to the issue of the origin of life in extraterrestrial environments and on the earth.

Among the small organic molecules present in the ISM, several nitriles have been identified (for a complete list, see, e.g., ref 1), including nitrile/isonitrile pairs (HCN/HNC, CH_3CN/CH_3NC, HCCCN/HCCNC), aliphatic saturated (CH_2CHCN, CH_3CH_2CN, n-/iso-propylcyanide) and unsaturated (in particular, the HC_nCN series with n = 0, 2, 4, ..., 10) nitriles, inorganic nitriles (MgCN, NaCN, and NH_2CN), as well as ions and unstable species (e.g., HNCCC, CN, HCCN, $HCNH^+$, HC_3NH^+, CH_2CN). However, the most interesting species containing the −CN− moiety are those that have a strong prebiotic character, such as cyanomethanimine and aminoacetonitrile (AAN, H_2NCH_2CN). The latter, detected toward the galactic center more than ten years ago,[16] is of particular interest in the framework of this study.

Despite the interest raised by the detection of AAN in the ISM, no energetically feasible gas-phase reactions have been suggested for the interstellar production of AAN. Indeed, in the last decade, grain-surface chemistry has been mostly invoked to explain the chemical complexity discovered in space, the basic idea being that when radical species trapped in icy mantles acquire some mobility, namely at temperatures above 30 K, they can combine and give rise to rich chemistry (see, e.g., refs 17−20). However, the recent observation of complex molecules also in very cold objects (at 10 K only H atoms are able to move around dust particles) has suggested that gas-phase reactions could have been overlooked.[3,21]

The reaction between an electrophilic radical and a molecule bearing an electron lone pair is expected to proceed with relative ease even in the harsh conditions of the ISM. In the present work, the electrophilic attack of the cyano radical on the nitrogen atom of methylamine has been thoroughly investigated through quantum-chemical calculations. As it will be shown, the reaction produces, via CN addition/H elimination, a large number of radical species of the general formula $C_2N_2H_5$, having either a CNCN or NCCN backbone,

$$CH_3NH_2 + CN \rightarrow [C_2N_2H_5] \rightarrow H_2NCH_2CN + H \quad (1)$$

These radicals, in turn, evolve toward a wealth of products, among which there are AAN, CH_2NH_2, and CH_3NH.

This specific reaction has been chosen because methylamine is the only amine detected till now in the ISM (both in the galactic center and outside).[22,23] At the same time, the CN radical is rather ubiquitous in astronomical environments, including interstellar molecular clouds,[24] comets,[25] and atmospheres of some planets and moons, like, e.g., Titan, the Saturn's largest moon. Above its haze, CN, after being generated from the photolysis of HCN, can react with olefins, leading to unsaturated nitriles.[26−29]

The manuscript is organized as follows: the computational methodology is described in Section 2, while the results are presented in Section 3. The latter section starts with a preliminary benchmark study to devise an accurate but cost-effective computational strategy to deal with complex reaction networks involving open-shell species and the problematic CN moiety; then, the reactive CH_3NH_2 + CN potential energy surface (PES) is investigated and the different reaction channels are discussed. Finally, conclusions and potential astrochemical implications are presented in Section 5.

2. COMPUTATIONAL DETAILS AND METHODOLOGY

On the grounds of previous studies,[30−33] a two-stage strategy was employed. The first step was a systematic analysis of the PES using the B3LYP hybrid functional[34,35] in conjunction with the SNSD basis set.[36] In the second step, the structures and relative stabilities of the stationary points located in the first step were refined by means of the double-hybrid B2PLYP functional[37,38] in conjunction with the maug-cc-pVTZ basis set[39] with d functions on hydrogen removed, namely, maug-cc-pVTZ-dH.[40] The dispersion effects, poorly described by semilocal density functionals,[41] were taken into account by means of the DFT-D3 scheme[42] employing the Becke−Johnson (BJ) damping function.[43] Indeed, the DFT-D3 model has been applied successfully to a large number of different systems, including dimers, supramolecular complexes, reaction energies/barriers, and surface processes (see, for example, refs 44−48 and references therein). To check the nature of the stationary points, as well as to obtain zero-point vibrational energy (ZPVE) corrections, harmonic vibrational frequency calculations were performed. Saddle points were assigned to reaction paths by using intrinsic reaction coordinate (IRC) calculations[49,50] for the identification of the corresponding reactants and products.

Subsequently, the energetics of all stationary points was accurately determined by applying the so-called "cheap" composite scheme[51−54] on top of B2PLYP-D3/maug-cc-pVTZ-dH optimized geometries. The starting point of this scheme is the electronic energy obtained at the coupled cluster (CC) level by employing the singles and doubles approximation augmented by a perturbative estimate of triples, CCSD(T),[55,56] in conjunction with the cc-pVTZ basis set[57] and within the frozen-core (fc) approximation. The fc-CCSD(T)/cc-pVTZ energy, $E_{elec}^{CCSD(T)/VTZ}$, is then corrected to account for the extrapolation to the complete basis set (CBS) limit as well as for core−valence correlation effect, according to the following equation

$$E_{elec}^{cheap} = E_{elec}^{CCSD(T)/VTZ} + \Delta E_{elec}^{CBS} + \Delta E_{elec}^{CV} \quad (2)$$

where ΔE_{elec}^{CBS} is the correction to the CBS limit and ΔE_{elec}^{CV} is the core−valence correlation contribution. To keep the computational cost low (hence the "cheap" denomination for this scheme), the corrective terms are evaluated by resorting to second-order Møller−Plesset perturbation (MP2) theory.[58] Going into detail, the extrapolation to the CBS limit is carried out by the n^{-3} equation[59] in conjunction with the cc-pVTZ and cc-pVQZ basis sets,[57] while the core−valence contribution is obtained as the energy difference between all electrons and fc MP2/cc-pCVTZ[60] calculations.

For comparison purposes, structures, energies, and harmonic force fields of all stationary points were also computed with the widely used CBS-QB3 composite method. While a detailed account can be found in ref 61, here we recall that it employs B3LYP/6-31G(d) geometries and harmonic force fields.

All of the calculations were performed with the Gaussian 16 quantum-chemical software[62] using, for open-shell species, restricted-open-shell Hartree−Fock (ROHF) wave functions but unrestricted Kohn−Sham orbitals.

3. RESULTS AND DISCUSSION

3.1. Validation of the Computational Protocol. In previous work,[63] two alternative paths for the addition of the CN radical to CH_3NH_2, namely, attack to the C and N ends,

https://dx.doi.org/10.1021/acsearthspacechem.0c00062
ACS Earth Space Chem. 2020, 4, 774−782

have been investigated using state-of-the-art computational protocols able to fulfill subchemical accuracy. In particular, a modification of the HEAT protocol,[64] referred to as "HEAT-like", was adopted to compute electronic energies, which were corrected for anharmonic ZPVEs computed using the B2PLYP-D3 functional. In that work, it was also demonstrated that the B2PLYP-D3/maug-cc-pVTZ-dH level of theory provides reliable molecular structures to be used as reference geometries in energetic evaluations of minima, reaction complexes, and radicals. However, the HEAT-like approach requires CC calculations involving the full treatment of triple and quadruple excitations as well as the evaluation of relativistic and diagonal Born−Oppenheimer corrections. Therefore, this protocol is too expensive for an extensive investigation of a reactive PES, as in the present case. For this reason, we resorted to the cheap protocol, whose accuracy has been preliminarily tested against the HEAT-like results for the species considered in the previous work. This comparison (see Table 1) demonstrates that the cheap protocol delivers remarkably accurate electronic energies for reaction intermediates, complexes, and also transition states, indeed showing a mean absolute deviation and a maximum deviation with respect to the HEAT-like values as small as 1.1 and −2.3 kJ mol^{-1}, respectively. Furthermore, it should be noted that according to the results reported in ref 63, the maximum error (0.4 kJ mol^{-1}) due to the employment of harmonic ZPVEs, in place of their more accurate anharmonic counterparts, is lower than the error due to the cheap protocol (in comparison to the HEAT-like value). Hence, unless otherwise stated, in the following, we will make explicit reference to cheap electronic energies corrected with harmonic B2PLYP ZPVE contributions.

Table 1. Comparison between Cheap and HEAT-like Relative Electronic Energies (kJ mol^{-1})

label ref 66	this work[a]	chemical formula	HEAT-like (ref 63)	cheap[b] this work
reactants	reactants	CH_3NH_2 + CN	0.0	0.0
FC01	n.a.	H_2NCH_2···HNC	−150.0	−151.8
RI	R16c	H_2NH_2CCNH	−187.4	−187.9
IC	IC01	H_3CH_2N···CN	−71.5	−73.5
FC02	FC01	H_3CHN···CHN	−127.6	−128.7
P1	P5	CH_2NH_2 + HCN	−133.4	−134.6
P2	P8	NH_2CH_2CN + H	−68.3	−69.6
P3	n.a.	CH_3NH + HCN	−100.9	−102.1
P4	n.a.	CH_3NHCN + H	−41.0	−42.3
P5	P3	NH_2CN + CH_3	−125.1	−127.4
TS0	n.a.	FC01 → RI	−112.8	-112.6
TS1	n.a.	RI → P1	−108.0	−107.8
TS2	TS12	RI → P2	−47.3	−47.8
TS3	TS1	IC → FC02	−31.3	−30.3
TS4	n.a.	IC → P4	31.9	31.8
TS5	n.a.	IC → P5	22.0	20.5
ME[c]				−0.9
MAE[d]				1.1
Max[e]				−2.3

[a]See also Figures 1 and 2; n.a. (not available) means that the species does not appear in the present work. [b]B2PLYP-D3/maug-cc-pVTZ-dH geometries. [c]Mean error with respect to HEAT-like reference values. [d]Mean absolute error with respect to HEAT-like reference values. [e]Maximum error with respect to HEAT-like reference values.

3.2. CH_3NH_2 + CN → [$C_2N_2H_5$] Reactive PES. As already pointed out, the CH_3NH_2 + CN reaction has previously been studied by our group to gain insights into the dichotomy between two competing channels, namely, the CN addition to the C and N ends of CH_3NH_2.[63] Furthermore, our previous work aimed at clarifying some inconsistencies between the experiment and theory.[65,66] There, it was found that abstraction from the CH_3 group proceeds through the formation of an initial prereactive complex that evolves to yield CH_2NH_2 and HCN as the main products, with a relative energy of −140.2 kJ mol^{-1} with respect to the reactant asymptote. In addition, a theoretical investigation of the rotational spectrum was carried out for the CH_2NH_2 radical (as well as for CH_3NH) to support its laboratory characterization. In the present study, we focus more deeply on the reaction path following the electrophilic attack of CN on the electron-rich nitrogen end of CH_3NH_2. Even though it is known that cyanates are more stable than isocyanates, initially, we also explored the possibility of the CN attack through the N atom. However, the addition complex (CH_3NH_2···NC) formed and the subsequent products (NH_2CH_2 and HNC) were found to be not only less stable but also involving quite high energy barriers. Therefore, this route was not considered further.

The theoretical investigation of the complete reaction mechanism has been undertaken starting from the initial addition complex IC01, lying 65.5 kJ mol^{-1} below the reactants (see Figure 1). The relative energies (in kJ mol^{-1}) obtained by different levels of theory are detailed in Table 2 and, for clarity and reader's convenience, the structures of all of the transition states are displayed in Figure 2, while those of the most relevant complexes and intermediates are illustrated in Figure 3. The equilibrium geometries of all the species optimized at the B2PLYP-D3/maug-cc-pVTZ-dH level are provided in the Supporting Information, together with cheap electronic energies and harmonic ZPVEs.

The B2PLYP-D3 results show the expected average deviations from more accurate computations. While they are not sufficient for a truly quantitative picture of the reaction energetics, they give further confidence in the reliability of the geometric parameters and harmonic frequencies obtained at this level.[67] In agreement with previous studies,[68] the results delivered by the widely employed CBS-QB3 model[61] are quite disappointing. Indeed, for some species (FC01, R12′, TS_{2-3}, P9), it shows discrepancies larger than 10 kJ mol^{-1} with respect to the cheap values, which, as discussed in the previous section, are close to very accurate benchmark values (see Table 1).

Moving to the reaction mechanisms, as previously shown,[63] FC01, more stable than the reactants by 133 kJ mol^{-1}, can decompose without any barrier to lead to CH_3NH + HCN. However, if an excess of energy is available and the first submerged barrier of 31 kJ mol^{-1} can be overcome, a sequence of radical species is then produced and can lead to prebiotic species such as AAN and some other nitrogen-containing molecules already identified in the ISM. Based on this assumption, we have thoroughly examined all possible intermediate radical species, final products, and the transition states interconnecting all of the above using the cheap scheme introduced above.

Chain reactions initiate with the rearrangement of FC01 to the very stable radical R1, thus overcoming a barrier of about ∼58 kJ mol^{-1} (TS2). Two alternative paths arise at this point.

https://dx.doi.org/10.1021/acsearthspacechem.0c00062
ACS Earth Space Chem. 2020, 4, 774−782

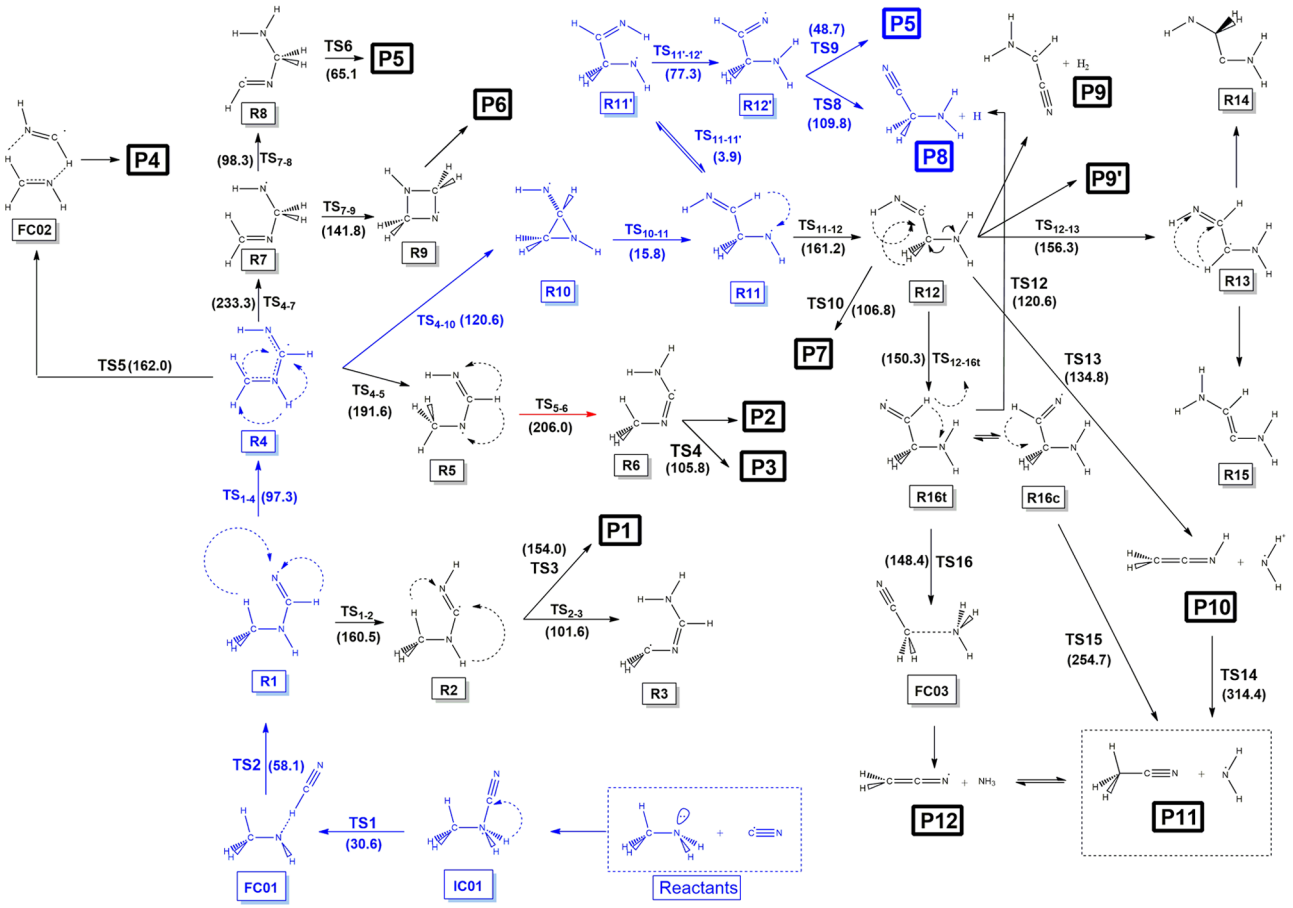

Figure 1. Schematic view of the CN addition reaction mechanism to CH_3NH_2. In parenthesis are the energy barriers (kJ mol^{-1}) calculated from the cheap electronic energies corrected for harmonic B2PLYP-D3/maug-cc-pVTZ-dH ZPVE. Highlighted in blue is the most probable pathway.

On the one side, a simple H-shift from carbon to nitrogen may occur ($TS_{1\text{-}2}$), with the radical R2 overcoming a quite high barrier (161 kJ mol^{-1}). In turn, R2 can evolve either to the very stable radical R3 through TS_{2-3} by two simultaneous H-shifts (overcoming a barrier of 102 kJ mol^{-1}) or to the product P1 through the transition state TS3. On the other side, a smaller barrier of about 97 kJ mol^{-1} (TS_{1-4}) favors, from the energetic point of view, the formation of R4 over the P1 product (i.e., CH_3NH + HNC).

The radical R4 is one of the key intermediates of the whole mechanism, as it discloses four different escape routes: three of them involve H-migrations and one involves cyclization. Based on energetic considerations, the latter is suggested to be the most favorable channel. As it can be seen from Figure 1 and Table 2, CH_2NH and HCNH (P4) directly form from the breaking of the H···N hydrogen bonds of complex FC02, after overcoming the energy barrier of 162 kJ mol^{-1} associated with the submerged transition state TS5. The reaction channels involving the generation of the radicals R5 and R7 appear closed under astronomical conditions because the transition states TS_{4-5} and TS_{4-7} (involving barriers of 192 and 233 kJ mol^{-1}, respectively) lie both above the reactants.

A more feasible path emerges through cyclization; indeed, a NH-substituted aziridine radical (R10) forms through the transition state TS_{4-10} (−64.4 kJ mol^{-1}), which exhibits a barrier of ∼121 kJ mol^{-1}. Next, the rearrangement of R10 into R11 ($NHCHCH_2NH$) occurs by overcoming the transition state TS_{10-11}, which involves a very small barrier of only 15.8 kJ mol^{-1}. Actually, the $NHCHCH_2NH$ radical exists in two different rotamers depending on the values of the NCCN dihedral angle: R11 corresponds to the gauche one (dihedral ∼140°), while R11′ is the cis conformer (dihedral ∼0°) and it is more stable by about 13 kJ mol^{-1}. These two radicals are involved in different pathways, thus leading to different products. Concerning R11, its possible chemical fate implies the conversion to R12 via the migration of a hydrogen atom from carbon to nitrogen. This is an energetically demanding process, with a barrier height of 161 kJ mol^{-1}, and it furthermore involves overcoming TS_{11-12}, which lies 38.1 kJ mol^{-1} above the reactants. In the case of R12, a number of possible exit channels would open, with the most straightforward option being the formation of CH_2NH_2 and HNC (P7). The corresponding TS10, which implies the breaking of the C−C bond, lies ∼51 kJ mol^{-1} below the reactants. Products P9 (NH_2CHCN + H_2) and P9′ ($NHCH_2CN$ + H_2), even if more stable than P7 (especially P9), seem to be less likely exit channels because they would imply the formation of a H_2 molecule from the coupling of two hydrogen atoms that, however, are located on C and N, thus being quite far apart. As a last option, R12 can lead to R16 (actually R16t, which is in conformational equilibrium with its rotamer R16c) that, in turn, can evolve toward either H_2CCN and NH_3 (P12) or CH_3CN and NH_2 (P11). In the former case, an intermediate step involves a submerged barrier of ∼148 kJ mol^{-1} and then leads to the final complex FC03 (−219.7 kJ mol^{-1}), whereas in the latter case the production of P11 directly follows from

https://dx.doi.org/10.1021/acsearthspacechem.0c00062
ACS Earth Space Chem. 2020, 4, 774−782

Table 2. Relative Energies (in kJ mol^{-1}) of All of the Species Involved in the CH_3NH_2 + CN Addition Reaction

name	chemical formula	E^0 (CBS-QB3)[a]	E^{el} B2PLYP	E^{el} cheap	ΔZPE	E^0 cheap[b]	barrier[b]
	CH_3NH_2 + CN	0.0	0.0	0.0	0.0	0.0	
IC01	CH_3NH_2···CN	−69.1	−89.9	−73.5	8.1	−65.5	
FC01	CH_3NH···HCN	−153.3	−145.6	−128.7	−4.8	−133.4	
FC02	CH_2NH···HCNH	−72.1	−82.3	−67.3	−3.1	−70.7	
FC03	CH_2CN···NH_3	−219.9	−229.7	−215.9	−3.8	−219.7	
R1	CH_3NHCHN	−176.1	−195.4	−182.3	11.1	−171.2	
R2	CH_3NHCNH	−178.9	−203.1	−185.6	10.2	−175.5	
R3	CH_2NCHNH_2	−218.0	−237.5	−220.3	7.6	−212.6	
R4	$CH_2NHCHNH$	−187.0	−208.2	−193.2	8.2	−185.0	
R5	CH_3NCHNH	−184.4	−195.0	−185.0	8.0	−177.0	
R6	CH_3NCNH_2	−176.9	−202.8	−182.1	10.0	−172.1	
R7	CH_2NCH_2NH	−113.1	−128.7	−115.8	6.5	−109.3	
R8	$CHNCH_2NH_2$	−133.1	−154.3	−141.3	11.4	−130.0	
R9	CH_2NCH_2NH (cyc)	−73.6	−89.5	−83.0	13.0	−70.0	
R10	$NHCH_2CHNH$(cyc)	−88.0	−102.2	−96.7	11.8	−84.9	
R11	$NHCHCH_2NH$	−127.9	−113.2	−135.0	11.9	−123.1	
R11′	$NHCHCH_2NH$	−135.4	−151.6	−143.7	7.9	−135.9	
R12	NH_2CH_2CNH	−159.0	−181.9	−170.4	12.4	−158.1	
R12′	NH_2CH_2CNH	−175.3	−188.5	−170.4	10.1	−160.4	
R13	$NH_2CHCHNH$	−243.5	−268.5	−253.9	13.1	−240.8	
R14	NH_2CCH_2NH	−6.4	−22.3	−14.3	14.7	0.4	
R15	NH_2CCHNH_2	−116.5	−141.4	−128.7	12.0	−116.7	
R16t	$NH_2CH_2CHNtrans$	−181.3	−195.0	−187.9	10.3	−177.6	
R16c	$NH_2CH_2CHNcis$	−179.9	−195.4	−189.2	10.3	−178.8	
TS1	IC01 → FC01	−28.4	−54.0	−30.3	−4.6	−34.9	30.6
TS2	FC01 → R1	−84.4	−89.1	−75.1	−0.2	−75.3	58.1
TS_{1-2}	R1 → R2	−11.2	−19.6	−7.2	−3.4	−10.7	160.5
TS3	R2 → P1	−20.1	−32.7	−17.7	−3.8	−21.5	154.0
TS_{2-3}	R2 → R3	−86.2	−87.1	−71.2	−2.8	−73.9	101.6
TS_{1-4}	R1 → R4	−77.2	−82.6	−71.6	−2.3	−73.9	97.3
TS_{4-5}	R4 → R5	0.8	0.8	10.6	−4.0	6.6	191.6
TS_{5-6}	R5 → R6	26.0	19.9	34.9	−5.8	29.0	206.0
TS4	R6 → P3	−71.9	−81.7	−62.9	−3.4	−66.3	105.8
TS5	R4 → FC02	−31.5	−39.6	−21.3	−1.7	−23.0	162.0
TS_{4-7}	R4 → R7	44.1	50.3	57.6	−9.4	48.3	233.3
TS_{7-8}	R7 → R8	−15.7	−14.9	−7.9	−3.1	−11.0	98.3
TS_{7-9}	R7 → R9	24.0	29.1	26.2	6.3	32.5	141.8
TS6	R8 → P5	−68.3	−82.5	−64.6	−0.3	−64.9	65.1
TS_{4-10}	R4 → R10	−71.0	−75.9	−71.4	7.0	−64.4	120.6
TS_{10-11}	R10 → R11	−75.3	−81.1	−77.3	8.3	−69.1	15.8
TS_{11-12}	R11 → R12	36.0	32.0	42.9	−4.8	38.1	161.2
$TS_{11-11'}$	R11 → R11′	−119.7	−133.6	−125.6	6.4	−119.2	3.9
$TS_{11'-12'}$	R11′ → R12′	−63.7	−66.4	−57.1	−1.5	−58.6	77.3
TS8	R12′ → P8	−55.7	−49.1	−40.4	−10.2	−50.6	109.8
TS9	R12′ → P5	−117.3	−127.3	−112.6	0.9	−111.7	48.7
TS10	R12 → P7	−54.8	−64.4	−47.4	−3.9	−51.3	106.8
TS_{12-13}	R12 → R13	0.2	−18.1	−1.5	−0.4	−1.8	156.3
TS_{12-16t}	R12 → R16t	−6.6	−13.7	−5.6	−2.2	−7.8	150.3
TS12	R16t → P8	−62.3	−59.7	−47.8	−9.2	−57.0	120.6
TS13	R12 → P10	−28.8	−43.1	−20.1	−3.2	−23.3	134.8
TS14	P10 → P11	217.3	224.5	245.8	18.1	263.9	314.4
TS15	R16c → P11	68.4	73.2	88.0	−12.1	75.9	254.7
TS16	R16t → FC03	−37.5	−42.6	−20.2	−9.0	−29.2	148.4
P1	CH_3NH + HNC	−54.2	−52.6	−40.5	−11.4	−51.9	
P2	CH_3NC + NH_2	−63.5	61.2	−48.2	−12.0	−60.2	
P3	NH_2CN + CH_3	−140.9	−139.1	−127.4	−16.1	−143.5	
P4	CH_2NH + HCNHt	−62.4	−66.3	−51.7	−8.3	−60.0	
P5	CH_2NH_2 + HCN	−140.8	−149.3	−134.6	−7.0	−141.6	
P6	CH_2NH + CH_2N	−97.5	−94.3	−82.5	−9.7	−92.2	
P7	CH_2NH_2 + HNC	−82.0	−84.9	−73.0	−8.4	−81.4	
P8	NH_2CH_2CN + H	−84.7	−79.6	−69.6	−14.2	−83.9	

https://dx.doi.org/10.1021/acsearthspacechem.0c00062
ACS Earth Space Chem. 2020, 4, 774−782

Table 2. continued

name	chemical formula	E^0 (CBS-QB3)[a]	E^{el} B2PLYP	E^{el} cheap	ΔZPE	E^0 cheap[b]	barrier[b]
P9	$NH_2CHCN + H_2$	−179.8	−166.8	−146.6	−23.2	−169.9	
P9′	$NHCH_2CN + H_2$	−94.6	−78.3	−63.5	−28.1	−91.5	
P10	$CH_2CNH + NH_2$	−49.4	−52.2	−34.3	−16.2	−50.5	
P11	$CH_3CN + NH_2$	−162.3	−164.7	−150.0	−12.0	−161.9	
P12	$CH_2CN + NH_3$	−210.1	−210.0	−198.8	−9.0	−207.7	

[a]ZPVE-corrected CBS-QB3 values. [b]Electronic energy from the cheap composite scheme corrected for harmonic B2PLYP-D3/maug-cc-pVTZ-dH ZPVE.

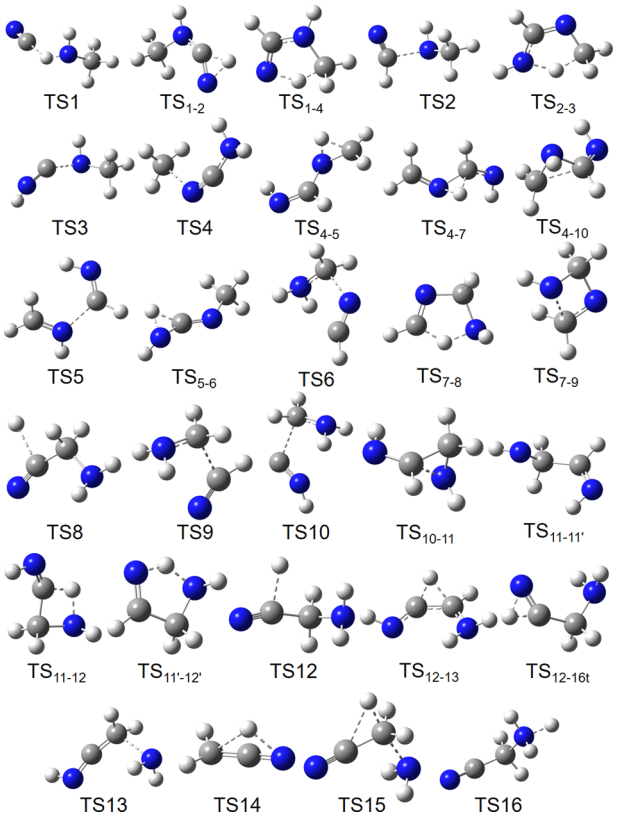

Figure 2. Structures of the transition states appearing in the scheme of Figure 1.

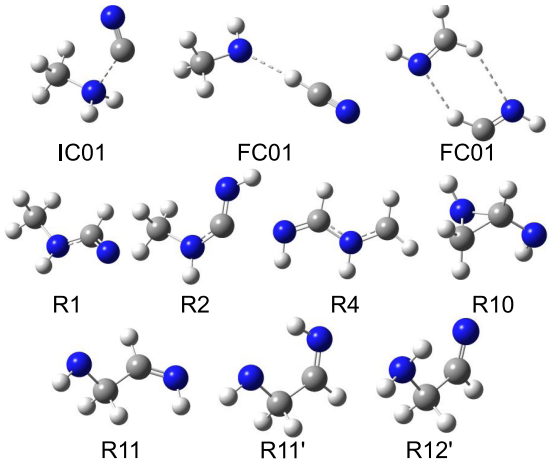

Figure 3. Structures of the most relevant complexes and intermediates appearing in the scheme of Figure 1.

R16c upon overcoming a barrier of ∼255 kJ mol^{-1} (TS15), which is indeed located 76 kJ mol^{-1} above the reactants. In passing, we note that R16t can lead to NH_2CH_2CN + H (P8). However, since TS_{11-12} is nonsubmerged, the paths following the formation of R12 and leading to P9, P9′, P10, P11, and P12 cannot be considered feasible under the conditions of the ISM; hence, the transition states involved in this portion of the PES have not been investigated in detail.

Finally, as previously mentioned, the $NHCHCH_2NH$ radical (R11) can be found in two conformers, depending on the NCCN dihedral angle. In the same way that R11 is transformed to R12 by passing through TS_{11-12}, R11′ should overcome the equivalent $TS_{11'-12'}$ for converting into R12′. Here, at variance with the path involving R11, not only R11′ and R12′ are more stable than the corresponding unprimed radicals by about 13 and 2 kJ mol^{-1}, respectively, but there is also a significant difference between the two transition states. In fact, while TS_{11-12} lies about 38 kJ mol^{-1} above the reactants and this translates to an energy barrier of 161 kJ mol^{-1}, $TS_{11'-12'}$ is submerged by 58.6 kJ mol^{-1}, lowering in this way the barrier to about 77 kJ mol^{-1}. Finally, from R12′ either CH_2NH_2 + HCN (P5) or NH_2CH_2CN + H (P8) can be formed by passing through the submerged transition states TS9 and TS8, respectively.

5. ASTRONOMICAL IMPLICATIONS AND CONCLUSIONS

Understanding the chemical evolution of extraterrestrial environments provides important insights into the composition of the organic matter, which, in turn, is the starting point for shedding light on the prebiotic chemistry occurring in the ISM and on planetary atmospheres. This requires the investigation of a large panel of reactions taking place among a number of possible reactants, which are generally selected among the species already detected. Nevertheless, in developing these complex reaction networks, gas-phase reactions are often overlooked, thus leading to the potential loss of important information.

The Strecker synthesis[69] is well known to lead to the formation of nitrile derivatives that, by hydrolysis, can evolve to amino acids. Among the different variants of this synthetic route, the simplest one is the formation of AAN, which eventually leads to glycine. While several theoretical studies have proven that aminoacetonitrile can be indeed formed by means of the Strecker synthesis,[70−74] a plausible formation route of AAN in the gas phase is now available. In fact, according to the reaction scheme reported in Figure 1 and the energetics detailed in Table 2, the products that, under astronomical conditions, can be formed from the addition of CN to the N atom of CH_3NH_2 are CH_3NH + HNC (P1), CH_2NH + HCNH (P4), CH_2NH_2 + HCN (P5), and NH_2CH_2CN + H (P8), all of them involving only submerged transition states and intermediates. Among these, in addition to hydrogen cyanide and hydrogen isocyanide, AAN[16] and

https://dx.doi.org/10.1021/acsearthspacechem.0c00062
ACS Earth Space Chem. 2020, 4, 774−782

CH_2NH[75] have already been detected in the ISM, and this is also the case for the $HCNH^+$ cation.[76,77] The first relevant branching point is R1 that can evolve either to R2 or R4. Based on energetic considerations, the second option appears preferable over the first one because it requires lower activation energy (97 kJ mol^{-1} for R1 → R4 vs 165 kJ mol^{-1} for R1 → R2). In an analogous way, it should be noted that from R4 the reaction requires overcoming a barrier of 162 kJ mol^{-1} to proceed toward P4, while for the path leading to P5 and P8, the highest energy barrier to overcome is about 120 kJ mol^{-1} (TS_{4-10}). Once R12′ is reached, the computed energies suggest that the formation of CH_2NH_2 + HCN is favored over that of AAN + H.

While the complexity of the pathway leading to AAN could make its formation unlikely to occur at extremely low temperatures (e.g., 10 K), in different environments, such as hot corinos or Titan's atmosphere, its feasibility cannot be excluded. As a matter of fact, according to the reaction scheme summarized in Figure 1, backward reactions from one intermediate to the previous one are not more favorable than the corresponding forward steps. However, the high stability of the R1, R4, R11′, and R12′ intermediates with respect to the final products suggests that these species might act as potential sinks for the overall reaction. In addition, the previous work on the reaction between CH_3NH_2 and CN has suggested that the competition between the CN attack to the C or N atoms of methylamine can also lead to the formation of the CH_3NH radical. Therefore, even if thermochemistry seems to be favorable, the appearance of the products P5 and P8, which are ∼142 and ∼84 kJ mol^{-1} more stable than the reactants, is not ensured from a kinetic point of view. However, because of the complexity of the pathway drawn in Figure 1, an exhaustive kinetic treatment is not straightforward, and work in this direction is in progress and will be the subject of a dedicated contribution.

Focusing on Titan's atmosphere, where the density is rather high with respect to the typical conditions of the ISM and third-body effects might help the reaction to occur, the reaction mechanism developed in this study suggests that AAN can be effectively formed. In this respect, the additional issue that might be raised is concerned with the reactants considered for the formation of AAN. While the CN radical is surely produced in Titan's atmosphere, the same does not apply to methylamine. However, its formation cannot be excluded since methanimine, i.e., its imine analogue, has already been detected.[78]

Overall, a large number of physicochemical parameters (e.g., activation energies, barriers, rate constants, reaction enthalpies, etc.) are required for modeling the complex network of elementary reactions taking place in extraterrestrial objects. Given the difficulty in performing experimental studies in the conditions relevant to astrochemistry, quantum-chemical calculations are often the only means to obtain such information, or to interpret experimental outcomes. However, to be successful, they should be as much accurate as possible. In this respect, this work has also confirmed the accuracy of the cost-effective composite model chemistry relying on cheap electronic energies computed on top of B2PLYP-D3/maug-cc-pVTZ-dH geometries. This methodology, tested against the results from a HEAT-like composite scheme, showed a mean absolute deviation around 1 kJ mol^{-1}. This outcome allows us to point out that the cheap approach is able to effectively deal with radical species and the pathological CN triple bond. Hence, it should be suggested as the method of choice to investigate complex reaction networks, such as those encountered in astrochemistry or atmospheric chemistry.

■ ASSOCIATED CONTENT

Supporting Information

The Supporting Information is available free of charge at https://pubs.acs.org/doi/10.1021/acsearthspacechem.0c00062.

Equilibrium geometries at B2PLYP-D3/maug-cc-pVTZ-dH level (Cartesian coordinates/Å), electronic energies from the cheap composite scheme (E^{el}/Hartree), harmonic zero-point vibrational energies at B2PLYP-D3/maug-cc-pVTZ-dH level (ZPVE/Hartree) (PDF)

■ AUTHOR INFORMATION

Corresponding Author

Nicola Tasinato − *Scuola Normale Superiore, 56125 Pisa, Italy;* orcid.org/0000-0003-1755-7238; Email: nicola.tasinato@sns.it

Authors

Zoi Salta − *Scuola Normale Superiore, 56125 Pisa, Italy;* orcid.org/0000-0002-7826-0182

Jacopo Lupi − *Scuola Normale Superiore, 56125 Pisa, Italy;* orcid.org/0000-0001-6522-9947

Rahma Boussessi − *Scuola Normale Superiore, 56125 Pisa, Italy*

Alice Balbi − *Scuola Normale Superiore, 56125 Pisa, Italy*

Cristina Puzzarini − *Department of Chemistry "Giacomo Ciamician", University of Bologna, 40126 Bologna, Italy;* orcid.org/0000-0002-2395-8532

Vincenzo Barone − *Scuola Normale Superiore, 56125 Pisa, Italy;* orcid.org/0000-0001-6420-4107

Complete contact information is available at: https://pubs.acs.org/10.1021/acsearthspacechem.0c00062

Notes

The authors declare no competing financial interest.

■ ACKNOWLEDGMENTS

This work was supported by the Italian MIUR under Grants 2015F59J3R (PRIN 2015, project "Simulation Tools for Astrochemical Reactivity and Spectroscopy in the Cyberinfrastructure", STARS in the CAOS) and 2017A4XRCA (PRIN 2017, project "Physico-chemical Heuristic Approaches: Nanoscale Theory of Molecular Spectroscopy", PHANTOMS), the University of Bologna (RFO funds), and Scuola Normale Superiore (grant number SNS18_B_TASINATO). The SMART@SNS Laboratory (http://smart.sns.it) is acknowledged for providing high-performance computing facilities.

■ REFERENCES

(1) McGuire, B. A. Census of Interstellar, Circumstellar, Extragalactic, Protoplanetary Disk, and Exoplanetary Molecules. *Astrophys. J., Suppl. Ser.* **2018**, *239*, 1−48.

(2) Chyba, C.; Sagan, C. Endogenous production, exogenous delivery and impact-shock synthesis of organic molecules: an inventory for the origins of life. *Nature* **1992**, *355*, 125−132.

(3) Balucani, N. Elementary reactions of N atoms with hydrocarbons: first steps towards the formation of prebiotic N-containing molecules in planetary atmospheres. *Chem. Soc. Rev.* **2012**, *41*, 5473−5483.

(4) Saladino, R.; Carota, E.; Botta, G.; Kapralov, M.; Timoshenko, G. N.; Rozanov, A. Y.; Krasavin, E.; Di Mauro, E. Meteorite-catalyzed syntheses of nucleosides and of other prebiotic compounds from formamide under proton irradiation. *Proc. Natl. Acad. Sci. U.S.A.* **2015**, *112*, E2746−E2755.
(5) Miao, Y.; Mehringer, D. M.; Kuan, Y.-J.; Snyder, L. E. Complex Molecules in Sagittarius B2(N): The Importance of Grain Chemistry. *Astrophys. J. Lett.* **1995**, *445*, L59−L62.
(6) Kuan, Y.-J.; Snyder, L. E. Three Millimeter molecular line observations of Sagittarius B2. II High resolution studies of $C^{18}O$, HNCO, NH_2CHO, and $HCOOHCH_3$. *Astrophys. J.* **1996**, *470*, 981−1000.
(7) Mehringer, D. M.; Menten, K. M. 44 GHz methanol masers and quasi-thermal emission in Sagittarius B2. *Astrophys. J.* **1997**, *474*, 346−361.
(8) Miao, Y.; Snyder, L. E. Full synthesis observations of CH_3CH_2CN in Sagittarius B2: Further evidence for grain chemistry. *Astrophys. J.* **1997**, *480*, L67−L70.
(9) Liu, S.-Y.; Mehringer, D. M.; Snyder, L. E. Observations of formic acid in hot molecular cores. *Astrophys. J.* **2001**, *552*, 654−663.
(10) Remijan, A.; Snyder, L. E.; Liu, S.-Y.; Mehringer, D.; Kuan, Y.-J. Acetic acid in the hot cores of Sagittarius B2(N) and W51. *Astrophys. J.* **2002**, *576*, 264−273.
(11) Snyder, L. E.; Lovas, F. J.; Mehringer, D. M.; Miao, N. Y.; Kuan, Y.-J.; et al. Confirmation of interstellar acetone. *Astrophys. J.* **2002**, *578*, 245−255.
(12) Tielens, A. G. G. M. The molecular universe. *Rev. Mod. Phys.* **2013**, *85*, 1021−1081.
(13) Endres, C. P.; Schlemmer, S.; Schilke, P.; Stutzki, J.; Müller, H. S. P. The Cologne Database for Molecular Spectroscopy, CDMS, in the Virtual Atomic and Molecular Data Centre, VAMDC. *J. Mol. Spectrosc.* **2016**, *327*, 95−104.
(14) Basiuk, V. A. Formation of Amino Acid Precursors in the Interstellar Medium. A DFT Study of Some Gas-Phase Reactions Starting with Methylenimine. *J. Phys. Chem. A* **2001**, *105*, 4252−4258.
(15) Herbst, E.; van Dishoeck, E. F. Complex Organic Interstellar Molecules. *Annu. Rev. Astron. Astrophys.* **2009**, *47*, 427−480.
(16) Belloche, A.; Menten, K. M.; Comito, C.; Müller, H. S. P.; Schilke, P.; Ott, J.; Thorwirth, S.; Hieret, C. Detection of amino acetonitrile in Sgr B2(N). *Astron. Astrophys.* **2008**, *482*, 179−196.
(17) Garrod, R. T.; Herbst, E. Formation of methyl formate and other organic species in the warm-up phase of hot molecular cores. *Astron. Astrophys.* **2006**, *457*, 927−936.
(18) Garrod, R. T. A three-phase chemical model of hot cores: the formation of glycine. *Astrophys. J.* **2013**, *765*, No. 60.
(19) Öberg, K. I.; Bottinelli, S.; Jorgensen, J. K.; van Dishoeck, E. F. A cold complex chemistry toward the low-mass protostar B1-b: Evidence for complex molecule production in ices. *Astrophys. J.* **2010**, *716*, 825−834.
(20) Linnartz, H.; Ioppolo, S.; Fedoseev, G. Atom addition reactions in interstellar ice analogues. *Int. Rev. Phys. Chem.* **2015**, *34*, 205−237.
(21) Taquet, V.; Wirström, E. S.; Charnley, S. B. Formation and recondensation of complex organic molecules during protostellar luminosity outbursts. *Astrophys. J.* **2016**, *821*, No. 46.
(22) Kaifu, N.; Morimoto, M.; Nagane, K.; Akabane, K.; Iguchi, T.; Takagi, K. Detection of interstellar methylamine. *Astrophys. J.* **1974**, *191*, L135−L137.
(23) Fourikis, N.; Tagagi, K.; Morimoto, N. Detection of interstellar methylamine by its $2_{02} \rightarrow 1_{10}A_a$-state transition. *Astrophys. J.* **1974**, *191*, L139−L141.
(24) Rodríguez-Franco, A.; Martin-Pinato, J.; Fuente, A. CN emission in Orion. The high density interface between the H_{II} region and the molecular cloud. *Astron. Astrophys.* **1998**, *329*, 1097−1110.
(25) Fray, N.; Bénilan, Y.; Cottin, H.; Gazeau, M.-C.; Croviser, J. The origin of the CN radical in comets: A review from observations and models. *Planet. Space Sci.* **2005**, *53*, 1243−1262.
(26) Wilson, E. H.; Atreya, S. K. Chemical sources of haze formation in Titan's atmosphere. *Planet. Space Sci.* **2003**, *51*, 1017−1033.
(27) Waite, J. H., Jr.; Young, D. T.; Cravens, T. E.; Coates, A. J.; Crary, F. J.; Magee, B.; Westlake, J. The Process of Tholin Formation in Titan's Upper Atmosphere. *Science* **2007**, *316*, 870−875.
(28) Lavvas, P. P.; Coustenis, A.; Vardavas, I. M. Coupling photochemistry with haze formation in Titan's atmosphere, Part II: Results and validation with Cassini/Huygens data. *Planet. Space Sci.* **2008**, *56*, 67−99.
(29) Morales, S. B.; Le Picard, S. B.; Canosa, A.; Sims, I. R. Experimental measurements of low temperature rate coefficients for neutral−neutral reactions of interest for atmospheric chemistry of Titan, Pluto and Triton: Reactions of the CN radical. *Faraday Discuss.* **2010**, *147*, 155−171.
(30) Spada, L.; Tasinato, N.; Vazart, F.; Barone, V.; Caminati, W.; Puzzarini, C. Noncovalent Interactions and Internal Dynamics in Pyridine−Ammonia: A Combined Quantum-Chemical and Microwave Spectroscopy Study. *Chem. - Eur. J.* **2017**, *23*, 4876−4883.
(31) Melli, A.; Melosso, M.; Tasinato, N.; Bosi, G.; Spada, L.; Bloino, J.; Mendolicchio, M.; Dore, L.; Barone, V.; Puzzarini, C. Rotational and Infrared Spectroscopy of Ethanimine: A Route toward Its Astrophysical and Planetary Detection. *Astrophys. J.* **2018**, *855*, No. 123.
(32) Li, W.; Spada, L.; Tasinato, N.; Rampino, S.; Evangelisti, L.; Gualandi, A.; Cozzi, P. G.; Melandri, S.; Barone, V.; Puzzarini, C. Theory Meets Experiment for Noncovalent Complexes: The Puzzling Case of Pnicogen Interactions. *Angew. Chem., Int. Ed.* **2018**, *57*, 13853−13857.
(33) Boussessi, R.; Ceselin, G.; Tasinato, N.; Barone, V. DFT meets the segmented polarization consistent basis sets: Performances in the computation of molecular structures, rotational and vibrational spectroscopic properties. *J. Mol. Struct.* **2020**, *1208*, No. 127886.
(34) Becke, A. D. Density-functional thermochemistry. III. The role of exact exchange. *J. Chem. Phys.* **1993**, *98*, 5648−5652.
(35) Lee, C.; Yang, W.; Parr, R. G. Development of the Colle-Salvetti correlation-energy formula into a functional of the electron density. *Phys. Rev. B* **1988**, *37*, 785−789.
(36) *Smartlab*. https://smart.sns.it/?pag=download.
(37) Grimme, S. Semiempirical hybrid density functional with perturbative second-order correlation. *J. Chem. Phys.* **2006**, *124*, No. 034108.
(38) Biczysko, M.; Scalmani, G.; Bloino, J.; Barone, V. Harmonic and Anharmonic Vibrational Frequency Calculations with the Double-Hybrid B2PLYP Method: Analytic Second Derivatives and Benchmark Studies. *J. Chem. Theory Comput.* **2010**, *6*, 2115−2125.
(39) Papajak, E.; Leverentz, H. R.; Zheng, J.; Truhlar, D. G. Efficient Diffuse Basis Sets: cc-pV*x*Z+ and maug-cc-pV*x*Z. *J. Chem. Theory Comput.* **2009**, *5*, 1197−1202.
(40) Fornaro, T.; Biczysko, M.; Bloino, J.; Barone, V. Reliable vibrational wavenumbers for C=O and N−H stretchings of isolated and hydrogen-bonded nucleic acid bases. *Phys. Chem. Chem. Phys.* **2016**, *18*, 8479−8490.
(41) Grimme, S. Density functional theory with London dispersion corrections. *WIREs Comput. Mol. Sci.* **2011**, *1*, 211−228.
(42) Grimme, S.; Anthony, J.; Ehrlich, S.; Krieg, H. A consistent and accurate ab initio parametrization of density functional dispersion correction (DFT-D) for the 94 elements H-Pu. *J. Chem. Phys.* **2010**, *132*, No. 154104.
(43) Grimme, S.; Ehrlich, S.; Goerigk, L. Effect of the Damping Function in Dispersion Corrected Density Functional Theory. *J. Comput. Chem.* **2011**, *32*, 1456−1465.
(44) Goerigk, L.; Grimme, S. A thorough benchmark of density functional methods for general main group thermochemistry, kinetics, and noncovalent interactions. *Phys. Chem. Chem. Phys.* **2011**, *13*, 6670−6688.
(45) Grimme, S. Supramolecular Binding Thermodynamics by Dispersion-Corrected Density Functional Theory. *Chem. - Eur. J.* **2012**, *18*, 9955−9964.
(46) Delle Piane, M.; Vaccari, S.; Corno, M.; Ugliengo, P. Silica-Based Materials as Drug Adsorbents: First Principle Investigation on

https://dx.doi.org/10.1021/acsearthspacechem.0c00062
ACS Earth Space Chem. 2020, 4, 774−782

the Role of Water Microsolvation on Ibuprofen Adsorption. *J. Phys. Chem. A* **2014**, *118*, 5801−5807.
(47) Tasinato, N.; Grimme, S. Unveiling the non-covalent interactions of molecular homodimers by dispersion-corrected DFT calculations and collision-induced broadening of ro-vibrational transitions: application to $(CH_2F_2)_2$ and $(SO_2)_2$. *Phys. Chem. Chem. Phys.* **2015**, *17*, 5659−5669.
(48) Tasinato, N.; Ceselin, G.; Stoppa, P.; Pietropolli Charmet, A.; Giorgianni, S. A Bit of Sugar on TiO_2: Quantum Chemical Insights on the Interfacial Interaction of Glycolaldehyde over Titanium Dioxide. *J. Phys. Chem. C* **2018**, *122*, 6041−6051.
(49) Fukui, K. The Path of Chemical Reactions — The IRC Approach. *Acc. Chem. Res.* **1981**, *14*, 363−368.
(50) Hratchian, H. P.; Schlegel, H. B. Theory and Applications of Computational Chemistry. In *The First 40 Years*; Dykstra, C. E.; Frenking, K.; Kim, S.; Scuseria, G., Eds.; Elsevier: Amsterdam, 2005; pp 195−249.
(51) Puzzarini, C.; Biczysko, M.; Barone, V.; Largo, L.; Peña, I.; Cabezas, C.; Alonso, J. L. Accurate Characterization of the Peptide Linkage in the Gas Phase: A Joint Quantum-Chemical and Rotational Spectroscopy Study of the Glycine Dipeptide Analogue. *J. Phys. Chem. Lett.* **2014**, *5*, 534−540.
(52) Puzzarini, C.; Biczysko, M. Microsolvation of 2-Thiouracil: Molecular Structure and Spectroscopic Parameters of the Thiouracil−Water Complex. *J. Phys. Chem. A* **2015**, *119*, 5386−5395.
(53) Spada, L.; Tasinato, N.; Bosi, G.; Vazart, F.; Barone, V.; Puzzarini, C. On the competition between weak O−H···F and C−H···F hydrogen bonds, in cooperation with C−H···O contacts, in the difluoromethane − *tert*-butyl alcohol cluster. *J. Mol. Spectrosc.* **2017**, *337*, 90−95.
(54) Alessandrini, S.; Puzzarini, C.; Barone, V. Extension of the "Cheap" Composite Approach to Noncovalent Interactions: The jun-ChS Scheme. *J. Chem. Theory Comput.* **2020**, *16*, 988−1006.
(55) Purvis, G. D., III; Bartlett, R. J. A full coupled-cluster singles and doubles model: The inclusion of disconnected triples. *J. Chem. Phys.* **1982**, *76*, 1910−1918.
(56) Raghavachari, K.; Trucks, G. W.; Pople, J. A.; Head-Gordon, M. A fifth-order perturbation comparison of electron correlation theories. *Chem. Phys. Lett.* **1989**, *157*, 479−483.
(57) Dunning, T. H., Jr. Gaussian basis sets for use in correlated molecular calculations. I. The atoms boron through neon and hydrogen. *J. Chem. Phys.* **1989**, *90*, 1007−1023.
(58) Møller, C.; Plesset, M. S. Note on an Approximation Treatment for Many-Electron Systems. *Phys. Rev.* **1934**, *46*, 618−622.
(59) Helgaker, T.; Klopper, W.; Koch, H.; Noga, J. Basis-set convergence of correlated calculations on water. *J. Chem. Phys.* **1997**, *106*, 9639−9646.
(60) Woon, D. E.; Dunning, T. H., Jr. Gaussian basis sets for use in correlated molecular calculations. V. Core-valence basis sets for boron through neon. *J. Chem. Phys.* **1995**, *103*, 4572−4585.
(61) Montgomery, J. A.; Frisch, M. J.; Ochterski, J. W.; Petersson, G. A. A Complete Basis Set Model Chemistry. VII. Use of the Minimum Population Localization Method. *J. Chem. Phys.* **2000**, *112*, 6532−6542.
(62) Frisch, M. J.; Trucks, G. W.; Schlegel, H. B.; Scuseria, G. E.; Robb, M. A.; Cheeseman, J. R.; Scalmani, G.; Barone, V.; Mennucci, B.; Petersson, G. A. et al. *Gaussian 16*, revision C.01; Gaussian, Inc.: Wallingford CT, 2016.
(63) Puzzarini, C.; Salta, Z.; Tasinato, N.; Barone, V.A twist on the reaction of the CN radical with methylamine in the interstellar medium: new hints from a state-of-the-art quantum-chemical study, *Astrophys. J.***2020**, submitted.
(64) Bomble, Y. J.; Vàzquez, J.; Kàllay, M.; Michauk, C.; Szalay, P. J.; Császár, A. J.; Gauss, J.; Stanton, J. F. High-accuracy extrapolated ab initio thermochemistry. II. Minor improvements to the protocol and a vital simplification. *J. Chem. Phys.* **2006**, *125*, 064108−1−064108-8.
(65) Sleiman, C.; El Dib, G.; Rosi, M.; Skouteris, D.; Balucani, N.; Canosa, A. Low temperature kinetics and theoretical studies of the reaction CN + CH_3NH_2: a potential source of cyanamide and methyl cyanamide in the interstellar medium. *Phys. Chem. Chem. Phys.* **2018**, *20*, 5478−5489.
(66) Sleiman, C.; El Dib, G.; Talbi, D.; Canosa, A. Gas Phase Reactivity of the CN Radical with Methyl Amines at Low Temperatures (23−297 K): A Combined Experimental and Theoretical Investigation. *ACS Earth Space Chem.* **2018**, *2*, 1047−1057.
(67) Vazart, F.; Latouche, C.; Cimino, P.; Barone, V. Accurate Infrared (IR) Spectra for Molecules Containing the C≡N Moiety by Anharmonic Computations with the Double Hybrid B2PLYP Density Functional. *J. Chem. Theory Comput.* **2015**, *11*, 4364−4369.
(68) Simmie, J. M.; Somers, K. P. Benchmarking Compound Methods (CBS-QB3, CBS-APNO, G3, G4, W1BD) against the Active Thermochemical Tables: A Litmus Test for Cost-Effective Molecular Formation Enthalpies. *J. Phys. Chem. A* **2015**, *119*, 7235−7246.
(69) Strecker, A. Ueber die künstliche Bildung der Milchsäure und einen neuen, dem Glycocoll homologen Körper. *Ann. Chem. Pharm.* **1850**, *75*, 27−45.
(70) Basiuk, V. A.; Bogillo, V. I. Theoretical Study of Amino Acid Precursor Formation in the Interstellar Medium. 1. Reaction of Methylenimine with Hydrogen Cyanide. *Adv. Space Res.* **2002**, *30*, 1439−1444.
(71) Basiuk, V. A.; Bogillo, V. I. Theoretical Study of Amino Acid Precursor Formation in the Interstellar Medium. 2. Reaction of Methylenimine with CN Radical. *Adv. Space Res.* **2002**, *30*, 1445−1450.
(72) Woon, D. E. Pathways to glycine and other amino acids in ultraviolet-irradiated astrophysical ices determined via quantum chemical modeling. *Astrophys. J.* **2002**, *571*, L177−L180.
(73) Koch, D. M.; Toubin, C.; Peslherbe, G. H.; Hynes, J. T. A Theoretical Study of the Formation of the Aminoacetonitrile Precursor of Glycine on Icy Grain Mantles in the Interstellar Medium. *J. Phys. Chem. C* **2008**, *112*, 2972−2980.
(74) Rimola, A.; Sodupe, M.; Ugliengo, P. Deep-space glycine formation via Strecker-type reactions activated by ice water dust mantles. A computational approach. *Phys. Chem. Chem. Phys.* **2010**, *12*, 5285−5294.
(75) Qin, S.-L.; Wu, Y.; Huang, M.; Zhao, G.; Li, D.; Wang, J.-J.; Chen, S. High-resolution submillimeter multiline observations of G19.61 − 0.23: Small-scale chemistry. *Astrophys. J.* **2010**, *711*, 399−416.
(76) Ziurys, L. M.; Turner, B. E. HCNH+: A New Interstellar Molecular Ion. *Astrophys. J.* **1986**, *302*, L31−L36.
(77) Ziurys, L. M.; Apponi, A. J.; Yoder, J. T. Detection of the quadrupole hyperfine structure in HCNH(+). *Astrophys. J.* **1992**, *397*, L123−L126.
(78) Vuitton, V.; Yelle, R. V.; Anicich, V. G. The nitrogen chemistry of Titan's upper atmosphere revealed. *Astrophys. J.* **2006**, *647*, L175−L178.

https://dx.doi.org/10.1021/acsearthspacechem.0c00062
ACS Earth Space Chem. 2020, 4, 774−782